SAND REPORT

SAND2003-0897
Unlimited Release
Printed March 2003

Status and Integrated Road-Map for Joints Modeling Research

Daniel J. Segalman, Thomas Paez, David Smallwood, Anton Sumali, and Angel Urbina

Prepared by
Sandia National Laboratories
Albuquerque, New Mexico 87185 and Livermore, California 94550

Sandia is a multiprogram laboratory operated by Sandia Corporation,
a Lockheed Martin Company, for the United States Department of Energy's
National Nuclear Security Administration under Contract DE-AC04-94-AL85000.

Issued by Sandia National Laboratories, operated for the United States Department of Energy by Sandia Corporation.

Available to DOE and DOE contractors from
U.S. Department of Energy
Of£ce of Scienti£c and Technical Information
P.O. Box 62
Oak Ridge, TN 37831

Telephone: (865) 576-8401
Facsimile: (865) 576-5728
E-Mail: reports@adonis.osti.gov
Online ordering: http://www.doe.gov/bridge

Available to the public from
U.S. Department of Commerce
National Technical Information Service
5285 Port Royal Rd
Spring£eld, VA 22161

Telephone: (800) 553-6847
Facsimile: (703) 605-6900
E-Mail: orders@ntis.fedworld.gov
Online ordering: http://www.ntis.gov/help/ordermethods.asp?loc=7-4-0#online

SAND2003-0897
Unlimited Release
Printed March 2003

Status and Integrated Road-Map for Joints Modeling Research

Daniel Segalman, David Smallwood, and Anton Sumali
Structrual Dynamics Research Department

Thomas Paez and Angel Urbina
Validation and Uncertainty Quantification Processes Department

Sandia National Laboratories
P.O. Box 5800
Albuquerque, NM 87185-0847
djsegal@sandia.gov

Abstract

The constitutive behavior of mechanical joints is largely responsible for the energy dissipation and vibration damping in weapons systems. For reasons arising from the dramatically different length scales associated with those dissipative mechanisms and the length scales characteristic of the overall structure, this physics cannot be captured adequately through direct simulation of the contact mechanics within a structural dynamics analysis.

The only practical method for accommodating the nonlinear nature of joint mechanisms within structural dynamic analysis is through constitutive models employing degrees of freedom natural to the scale of structural dynamics. This document discusses a road-map for developing such constitutive models.

Acknowledgment

The author list includes only those people who have actually contributed text and figures to this road map. Many additional people have contributed to the plans described. These include people formally on the joints team - experimentalists, analysts, and model developers - as well as others who have a stake in the exploitation of these models. Some of those people also provided critical review of this document and helpful suggestions. Among those who should be recognized in particular are Fernando Bitsie, Dan Gregory, Ron Hopkins, Todd Simmermacher, and Howard Walter.

Two external parties need to be recognized as well. The joints research effort under Prof. Lawrence Bergman at the University of Illinois has contributed to the foundations of much of the plan presented here. In particular, they demonstrated that "whole-interface" elements can capture transient response of jointed structures. Collaborative work with Prof. Dane Quinn of the University of Akron has lead to at least one candidate constitutive model for the special interface approach discussed here.

Additionally those managers who have supported the joints research effort over the last several years deserve an expression of appreciation. First among these is David Martinez, who provided moral and budgetary support at the inception of this project. He was also an indefatigable advocate during those crucial years. Also to be credited is Jaime Moya who not only provided advocacy for the joints program, but has also funded an expanding experimental effort which provides a fundamental foundation for the modeling program. There are several more managers who have provided support for the joints effort in recent years, these include Justine Johannes, Hal Morgan, and Jim Redmond. Jim's efforts in coordinating the overall joints research program and helping transition it to the users are a major and continuing asset to the research program.

Contents

Figures

This page intentionally left blank

Status and Integrated Road-Map for Joints Modeling Research

Introduction

In the context of the research plan presented here, joint mechanics refers to the mechanical properties of joints commonly found in weapons systems and their impact on the structural response of the systems of which they are a part. The mechanics of interest are usually manifest as non-linear vibration damping, non-linear stiffness, or a transfer of mechanical energy from low frequency to high. All of these manifestations must be accounted for in the prediction of structural response of weapons systems, but no appropriate constitutive models for these phenomena exist as of now. It is the purpose of the research planned out here to develop and implement such models.

The broad range of joint mechanisms and the hardware environments in which they are manifest requires that the research and modeling effort be strategically staged. It is envisioned that mechanisms will be addressed with tools of increasing sophistication and that emphasis will shift from one mechanism to another, as the first come under control. This document will discuss the research and modeling directions that are envisioned, and roughly the order in which they will be pursued.

Necessity of Joint Models

The constitutive behavior of mechanical joints is largely responsible for the energy dissipation and vibration damping in weapons systems. For reasons arising from the dramatically different length scales associated with those dissipative mechanisms and the length scales characteristic of the overall structure, this physics cannot be captured through direct simulation of the contact mechanics within a large-scale structural dynamics analysis. The difficulties manifest themselves either in terms of Courant times orders of magnitude smaller than that necessary for structural dynamics analysis or they may manifest themselves as intractable problems associated with matrices of extraordinarily large condition number.

For instance, consider a crude solid-element model for an RV employing approximately 10^6 degrees of freedom. If the smallest element dimension is about 0.25

centimeter and has properties similar to aluminum, the maximum allowable time step for explicit integration will be on the order of 10^{-7} seconds. If we add fifty appropriately meshed joints, each having approximately 10^6 degrees of freedom, the total number of degrees of freedom is still manageable. The intractable problem is that to capture the micro-mechanics that govern joint response, the elements must be on the order of 10^{-3} cm and the minimum time step is on the order of 4×10^{-10} seconds. This minimum time step makes practical calculations in reasonable time impossible. If this integration is performed implicitly, the difficulty is manifest as matrix ill-conditioning.

The only practical method for accommodating the nonlinear nature of joint mechanisms within structural dynamic analysis is through constitutive models employing degrees of freedom natural to the scale of structural dynamics. In this way, development of constitutive models for joint response is a prerequisite for a predictive structural dynamics capability.

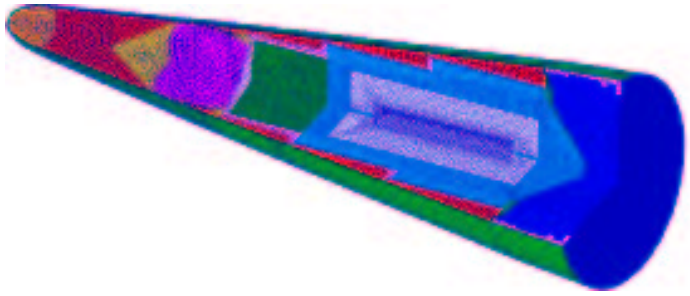

Figure 1. *Fine mesh finite element analysis can handle millions of degrees of freedom where interfaces are not an issue.*

Joint Mechanisms

There are two canonical joint mechanisms typically encountered in structural vibrations. They are commonly referred to as "slip" and "slap" processes, illustrated in Figures 2 and 3.

Each process influences structural dynamic response in its own distinct manner. Slip processes introduce additional flexibility at high loads, but more importantly, slip is associated with energy dissipation that serves to moderate vibration amplitude.

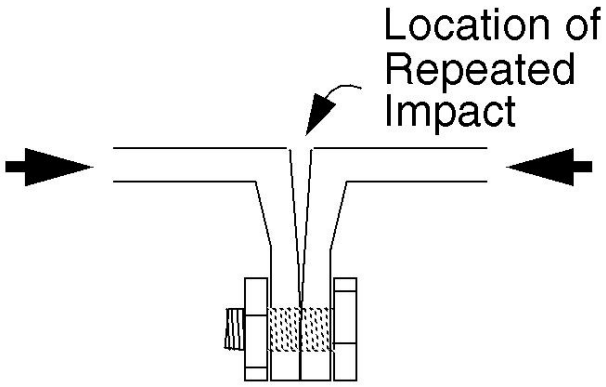

Figure 2. *Slap processes both dissipate energy and transfer energy from low to high frequency.*

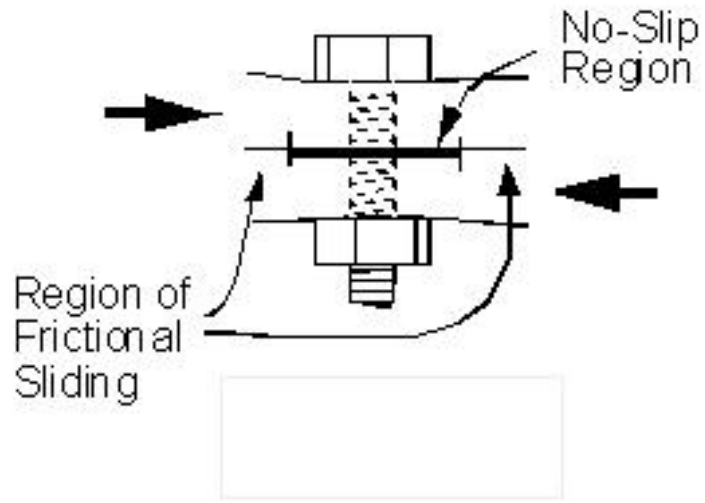

Figure 3. *Slip processes dissipate energy at bolted or press-fit connections.*

Slap processes occur at high vibrational amplitudes, when near-by portions of the structure are brought into dynamic contact. Because impulses contain all frequency components (the Fourier expansion of a Dirac delta function has finite amplitude out to infinite frequency) slap processes transfer energy to higher frequencies than those that excite the slap process.

Each of these processes is fundamentally nonlinear and introduces nonlinearity into the dynamic response of the structures of which they are a part. It is the purpose of the work outlined here to devise methods to model joint behavior and to integrate those models into the larger models for the dynamics of structures.

Also, each of these processes are extremely difficult to measure - or even examine - directly. Until loads are sufficient to induce macro-slip, the slip-related kinematics of the joints are substantially smaller than the elastic deformations of the surrounding structure. It is only once loads reach levels necessary to cause macro-slip, that any joint related kinematics can be measured. These difficulties were identified more than fifty years ago [11]. It is discussed below how, though joint mechanisms cannot be measured directly, insight can be obtained by examining some integrated structural response - in particular energy dissipation.

Similarly, dynamic gapping/slapping processes are difficult to observe and measure directly, but can be explored indirectly through study of some integrated properties of the structures in which they occur.

The above questions of what can be observed directly also impact the validation program. There too, one must devise techniques that rely on indirect measures of joint response such as energy dissipation, ring-down, or resonant frequency shift. (See Section)

Qualitative Properties of Slip-Related Joint Mechanics

The qualitative properties of a lap-type joint (Figure 3) are illustrated in Figure 4. Under small loads, the joint displacement appears linear, though we know via load reversals that there is some nonlinear hysteresis in that regime. As monotonic loads are applied and increased, the magnitude of slip increases and the force-displacement curve begins to bend over (soften). Eventually, when the applied force is sufficient to cause macro-slip, the curve becomes level. Whether the slope of the force-displacement curve is continuous at the inception of macro-slip, is an open question. If the joint

contains a bolt or other constraint that prevents indeterminate joint displacement, the period of macro-slip is very short. Once the macro-slip has exceeded the tolerance of the bolt in its hole, the force-displacement curve will reflect the elastic deformations of the bolt and the bodies it connects. At that stage, the curve will take on a linear nature reflecting the uni-directional elasticity of those components.

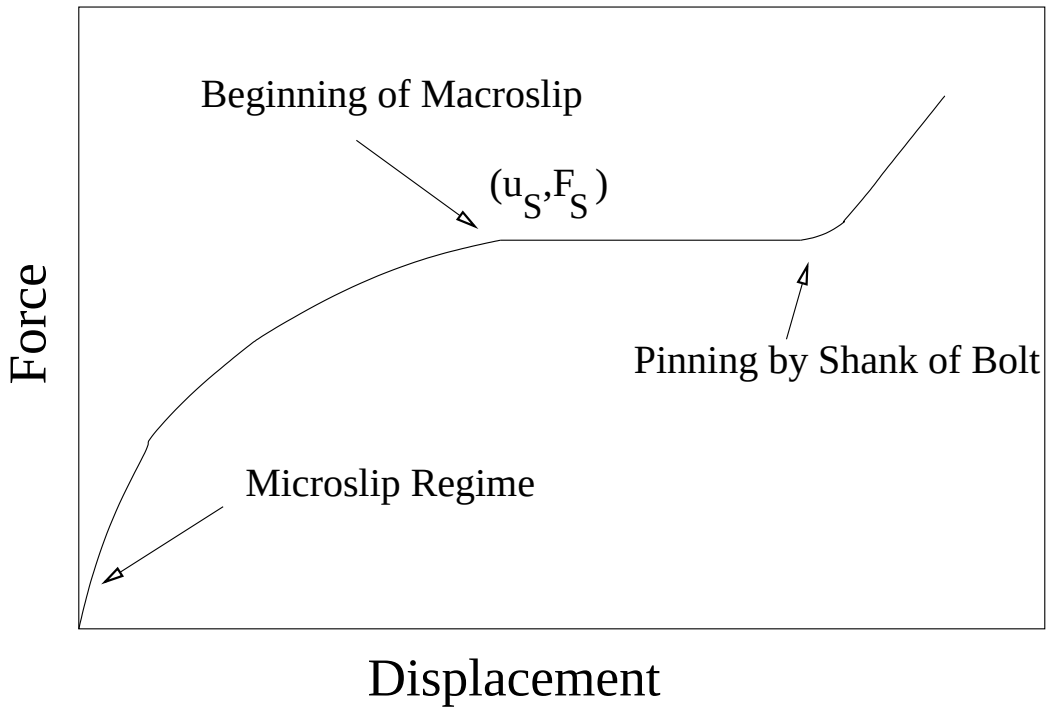

Figure 4. *The monotonic pull of a simple lap joint shows the force saturates at F_S as the displacement passes a critical value.*

The previous section alluded to the difficulty of directly observing slip mechanisms. Joint mechanics are obscured in macroscopically measured forces and displacements by the much larger elastic deformations of the structure. Figure 5 demonstrates the large elastic deformation, primarily bending, that results when a simple lap joint is subject to extension under two different pairs of boundary conditions.

The manner in which elastic deformations obscure the joint mechanics is illustrated in Figure 6 for the same problem. We see that initially, almost all of the deformation is that associated with elastic bending and only a small amount is micro-slip taking place at the joint. Once the force exceeds that necessary to initiate macro-slip, all

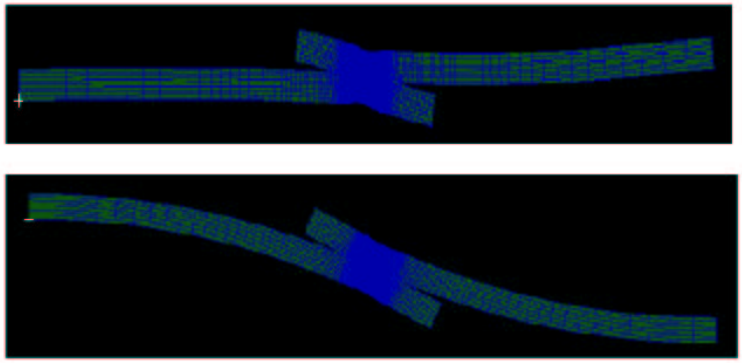

Figure 5. *The monotonic pull of a simple lap joint shows substantial bending. The top image indicates the deformation predicted by quasi-static nonlinear finite element analysis (Abaqus) when both sides are cantilevered and then extended. The figure on the bottom is cantilevered on the left and held by rollers on the right.*

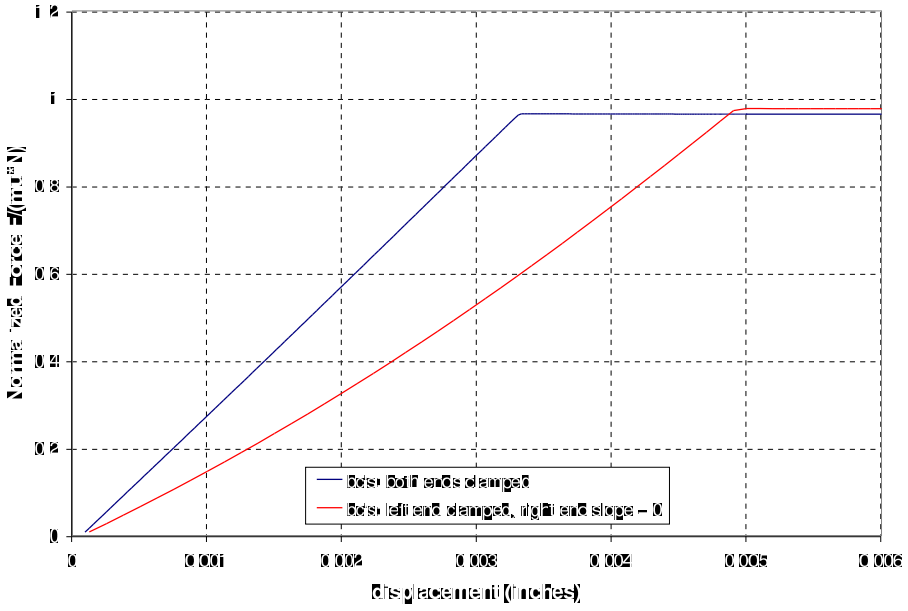

Figure 6. *The displacements on the right hand sides of the specimens of Figure 5 when subject to monotonic pull. Initially, almost all of the deformation is that associated with elastic bending. Once the force exceeds that necessary to initiate macro-slip, all the incremental deformation is due to the joint.*

the incremental deformation is due to the joint. The only element of this experiment that relates directly to joint response is the force F_S necessary to initiate macro-slip. The above is consistent with our current qualitative understanding of lap joints.

An entirely different sort of experiment is necessary to obtain more resolution on the slip mechanisms of the joint. One class of experiment is that pioneered by Gaul ([3], [4], and [5]) and improved by Gregory *et. al.* ([6], [15]). That class involves imposing harmonic loads on the jointed structure and deducing energy dissipation per cycle. Since the joint is the only source of energy dissipation in the jointed structure, all of the dissipation must be assigned to the joint. (Experiments with monolithic test specimens confirm that there is no significant dissipation taking place elsewhere in the testing apparatus.) Because the level of dissipation per cycle is small compared to the peak elastic energy of the system, sophisticated signal processing tools and many cycles must be employed to obtain the desired dissipation information.

Characteristically the energy dissipation appears to behave as a power of the amplitude of the harmonic driving force until the force amplitude approaches the macro-slip force F_S. Figure 7 shows the general form of the dissipation function that one finds experimentally. There are some solutions to classical elastic-contact problems that yield a log-log slope of exactly 3.0, but experimental data almost always seems to define curves of slope between 2.0 and 3.0, represented as $3 + \chi$ where χ is a small negative number $-1 < \chi < 0$. There are multiple plausible explanations for the fractional power-law relationship found experimentally. One such explanation will be discussed in a later section of this report.

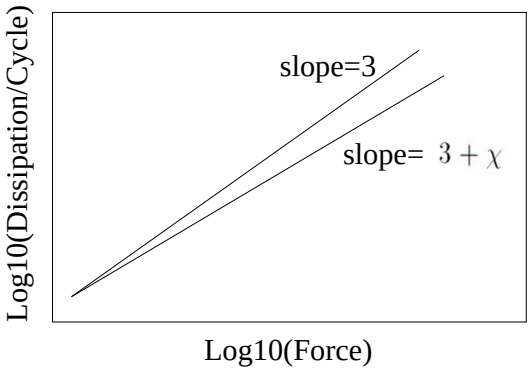

Figure 7. *The dissipation per cycle in a harmonically loaded jointed structure appears to be a fractional power of the amplitude of the applied force. (See text.)*

An example of energy dissipation in steady state harmonic excitation is that of Dan Gregory's experiment on a bolted leg (Figure 8) of a mock W76 arming-fusing-firing (AFF) assembly. The dissipation as a function of force amplitude is indicated in Figure 9. In this case the dissipation slope is approximately 2.4 ($\chi = -0.6$). It is interesting that despite some variability from experiment to experiment, there is little variability in the slope.

Goals of Joints Modeling

As one would expect from the complexity of the joint mechanisms, there is tremendous part-to-part variability in all experimental joint data. In this context, a successful joint model must generate predictions that lie within a cloud of data representing the uncertainty of the true situation. Further, a successful model should have the ability to say something about uncertainty:

- ideally, a successful modeling process could map small variations in boundary conditions or surface conditions to corresponding variability in the model parameters
- a knowledge of uncertainty associated with each joint should map to quantifiable uncertainty in the larger structure of which the joint is a part.
- indeed, a joint model might be used in an intrinsically probabilistic manner. For instance, in simulating a structure with many similar joints, one might assign joint parameters in a random manner consistent with anticipated probability distributions.

Whole-Interface Models for Lap-Type Joints

The goal is to capture the joint response with reasonable fidelity in a manner that can be incorporated into structural-level finite element code. The first effort to achieve this goal involves generating the simplest models that can reproduce the experimental results. The approach selected for this purpose is referred to here as a "whole-interface" approximation:

- The portion of each body near an interface is constrained so that all the nodes on that side of the interface move rigidly together

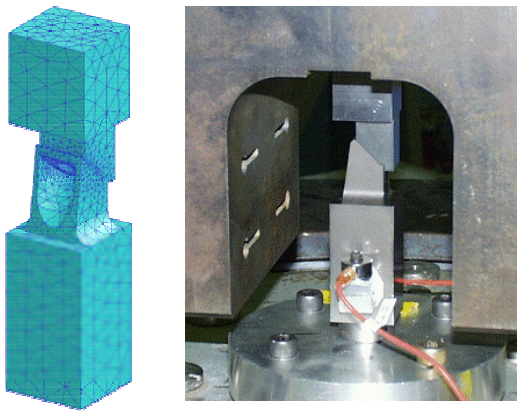

Figure 8. *The mock W76 AFF bolted joint and a finite element mesh used to simulate that joint.*

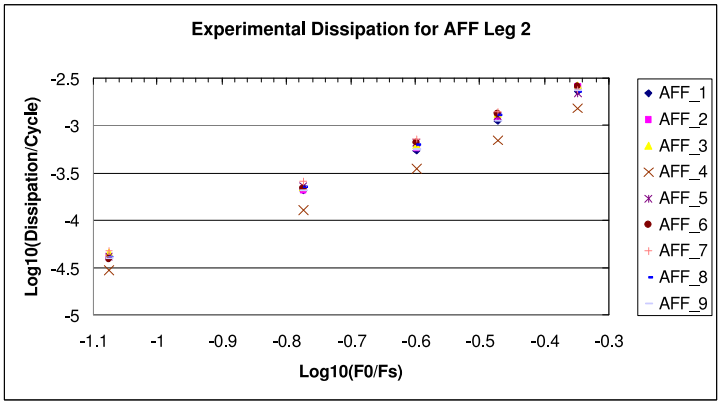

Figure 9. *The dissipation per cycle in a harmonically loaded jointed structure appears to be a fractional power of the amplitude of the applied force. The experimental data shown is from nine different but nominally identical lap joints (AFF_1, AFF_2, ...).*

- Those mutually constrained nodes are tied to a single node located approximately at the center of the region of contact
- Each of the six degrees of freedom of the opposing nodes are connected to the corresponding degrees of freedom of the opposite node by a scalar equation.

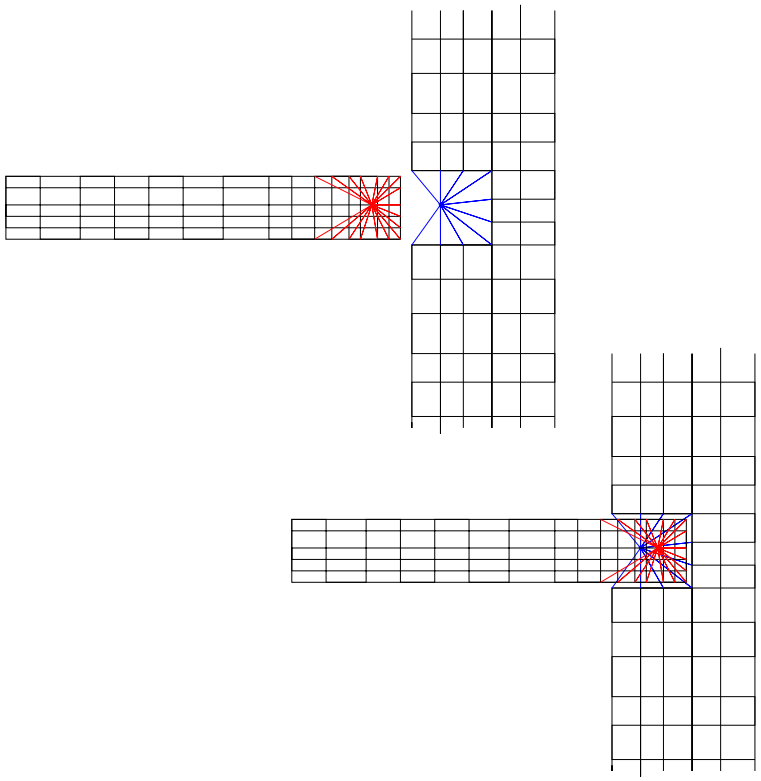

Figure 10. *The "whole-interface" approach to simulation of joints reduces the number of degrees of freedom at a joint to one in the direction of each degree of freedom. This approach would be applied to generalized lap-type joints, including compression fits such as shown here.*

The degrees of freedom associated with dissipation are connected by nonlinear scalar constitutive equations capable of reproducing the observed experimental dissipation and manifesting macro-slip at the appropriate load level. The remaining degrees of freedom are connected by an elastic spring. This approach would be appropriate to a generalized class of 'lap-type' joints, including compression joints such as shown in Figure 10.

CURRENT STATUS OF WHOLE-JOINT MODELING

- All of the scalar equations are assumed to be independent.
- Two classes of nonlinear constitutive equation appropriate for *whole-interface* modeling have been developed. These are Dave Smallwood's power-law hysteresis model [16] and Segalman's ([13] & [14]) class of Iwan model.
- Both of those constitutive models have been implemented in the Salinas structural dynamics finite element code.

PLANNED RELATED ACTIVITIES

- It is anticipated that the loads associated with hostile environments - such a potentially seen in the Stockpile-to-Target-Sequence (STS) - would exceed those necessary to initiate macro-slip. An extension of the above formulation to accommodate such loads will be necessary. Also necessary to accommodate such environments will be accounting for time-varying normal loads. A strategy exists for dealing with these conditions in the context of Iwan models, but a time-line for implementation has not yet been set.
- An effort has been initiated to couple the nonlinear equations for the shear degrees of freedom. It is envisioned that this coupling will be analogous to that of flow surfaces in multi-dimensional plasticity.

  A version of this coupled *whole-interface* formulation is targeted for third quarter FY04.

Iwan Modeling

To be useful, such constitutive models must have the following properties:

- They must be capable of reproducing the important features of joint response - dissipation and nonlinear stiffness.
- There must be a systematic method to deduce model parameters from joint-level experimental data or from very fine scale quasi-static, nonlinear finite element modeling of the joint region. (There are associated questions of the validation of that finite element code for each class of joint.)

- Integration into a structural-level finite element code must be practical.

A framework that has potential for providing that balance is that due to Iwan (1967,1968) and the work reported here addresses how that model-form can be exploited to capture the important responses of mechanical joints.

Iwan introduced constitutive models for metal elasto-plasticity that have since been used in joint modeling. Of his models, the most prominent has been the parallel system of Jenkins elements, sometimes called the parallel-series Iwan model. As the name implies, such models consist of spring-slider units arranged in a parallel system as indicated in Figure 11.

Mathematically, the constitutive form of the model is (Segalman, 2001)

$$F(t) = \int_0^\infty \rho(\phi)[u(t) - x(t,\phi)]\, d\phi \tag{1}$$

and

$$\dot{x}(t,\phi) = \begin{cases} \dot{u} & \text{if } \|u - x(t,\phi)\| = \phi \\ 0 & \text{if } \|u - x(t,\phi)\| < \phi \end{cases} \tag{2}$$

We are now guaranteed that $\|u - x(t,\phi)\| \leq \phi$. In the above, ϕ is a break-free force and $\rho(\phi)$ is the population density of spring-slider pairs where the slider has strength ϕ.

The parameter k was removed from the formulation through an appropriate change of variables (Segalman, 2002). This change of variables alters the dimensions of the remaining model parameters: ϕ has dimensions of Length and ρ has dimensions of Force/Length^2.

Two overall parameters for the interface can be expressed in terms of the above integral system. The force necessary to cause macro-slip (slipping of the whole interface) is denoted F_S and the stiffness of the joint under small applied load (where slip is infinitesimal) is denoted K_T. For the parallel-series Iwan system, macro-slip is characterized by every element sliding:

$$u(t) - x(t,\phi) = \phi \tag{3}$$

for all ϕ, so Equation 1 yields

$$F_S = \int_0^\infty \phi\rho(\phi)\, d\phi \tag{4}$$

Similarly for the parallel-series Iwan system, no elements have slid at the inception of loading,

$$x(t,\phi) = 0 \tag{5}$$

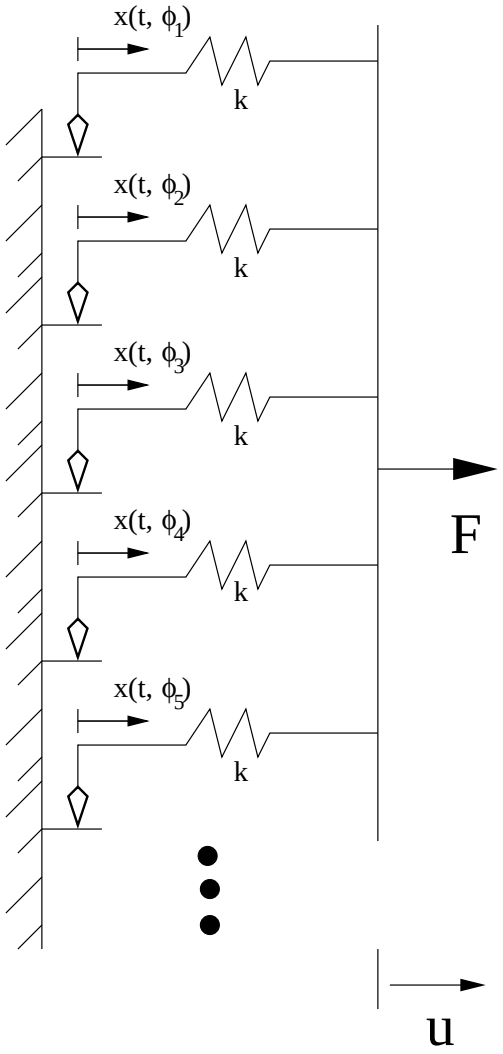

Figure 11. *A parallel-series Iwan system*

at $t = 0$, so Equation 1 yields

$$K_T = \int_0^\infty \rho(\phi)\, d\phi \tag{6}$$

If the joint is subject to cyclic oscillatory deformation, the slope of the hysteresis curve just after reversal has the value K_T. (See Figure 12.)

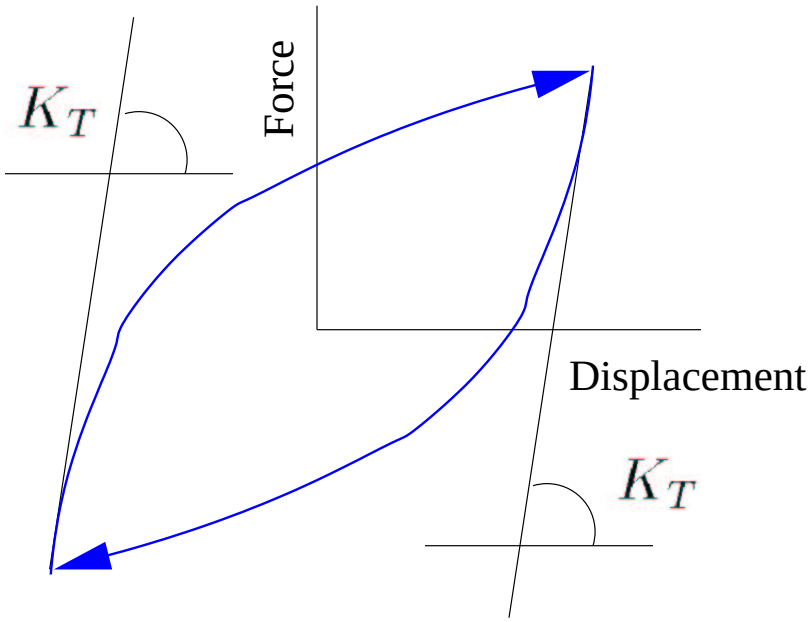

Figure 12. *The joint parameter K_T is the slope of the hysteresis curve immediately after a force reversal.*

We are lead to consider parallel Iwan systems (Segalman, 2002) having a power-law population distribution terminated by a Dirac delta:

$$\rho(\phi) = R\phi^\chi[H(\phi) - H(\phi - \phi_{\max})] + S\delta(\phi - \phi_{\max}) \tag{7}$$

where $H()$ is the Heaviside step function and $\phi_{\max}$ is numerically equal to u_s, the joint displacement at which micro-slip transitions into macro-slip. The coefficient S has a value to bring the slope of the monotonic pull curve down to zero at (u_s, F_s). This form of population distribution is shown graphically in Figure 13.

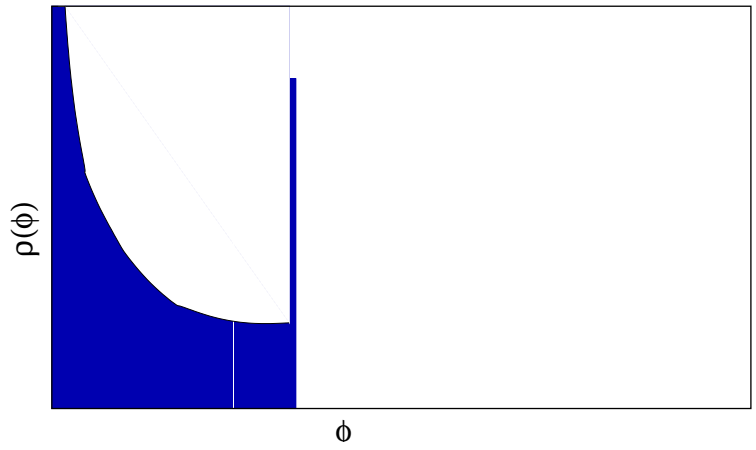

Figure 13. *A spectrum that is the sum of a truncated power law distribution and a Dirac delta function can be selected to satisfy asymptotic behavior at small and large force amplitudes.*

Substitution of Equation 7 into Equation 1 yields

$$F(t) = \int_0^{\phi_{\max}} [u(t) - x(t,\phi)] R\phi^{\chi}\, d\phi + S[u(t) - x(t,\phi_{\max})] \tag{8}$$

Equation 2 remains unaltered.

The macro-slip force for the system becomes

$$\begin{aligned} F_S &= \int_0^{\phi_{\max}} \phi\rho(\phi) d\phi && (9)\\ &= \frac{R\phi_{\max}^{\chi+2}}{(\chi+2)} + S\phi_{\max} && (10)\\ &= \phi_{\max}\left(\frac{R\phi_{\max}^{\chi+1}}{\chi+1}\right)[\frac{\chi+1}{\chi+2} + \beta] && (11) \end{aligned}$$

where

$$\beta = S/\left(\frac{R{\phi_{\max}}^{\chi+1}}{\chi+1}\right) \tag{12}$$

Because χ and β are dimensionless and because F_S can be measured or computed fairly directly, a preferred set of model parameters are $\{\chi, \beta, F_S, \phi_{\max}\}$. For this

reason, one inverts Equation 11 to solve for R and employs Equation 12 to express S appropriately:

$$R = \frac{F_S(\chi+1)}{\phi_{\max}^{\chi+2}\left(\beta + \frac{\chi+1}{\chi+2}\right)} \tag{13}$$

and

$$S = \left(\frac{F_S}{\phi_{\max}}\right)\left(\frac{\beta}{\beta + \left(\frac{\chi+1}{\chi+2}\right)}\right) \tag{14}$$

The interface stiffness can be computed as

$$K_T = \int_0^{\phi_{\max}} \rho(\phi)d\phi = \frac{R\phi_{\max}^{\chi+1}}{(\chi+1)} + S = \frac{R\phi_{\max}^{\chi+1}}{(\chi+1)}(1+\beta) = \frac{F_S(1+\beta)}{\phi_{\max}(\beta + \frac{\chi+1}{\chi+2})} \tag{15}$$

Processes to deduce model parameters suitable to match experimental curves for dissipation are given by Segalman [14]. Sample fits to experimental data are shown in Figure 14 for the mock W76 AFF leg and Figure 16 for a stepped joint.

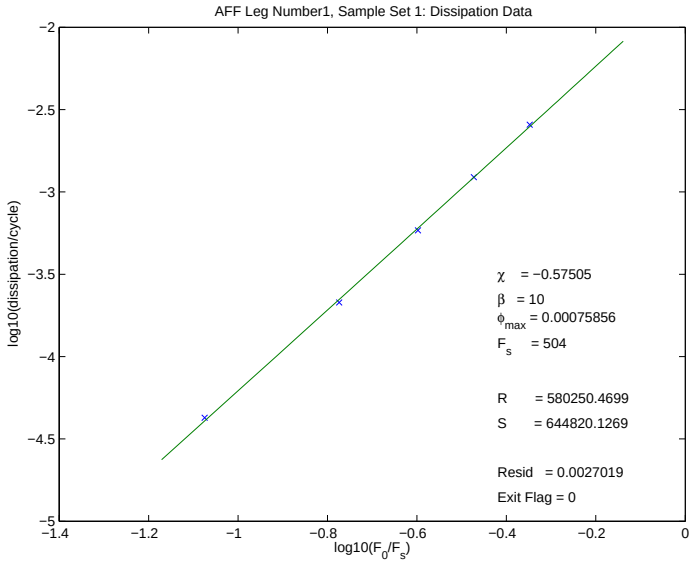

Figure 14. *Fit to dissipation data from a mock W76 AFF leg using an optimization method within Matlab.*

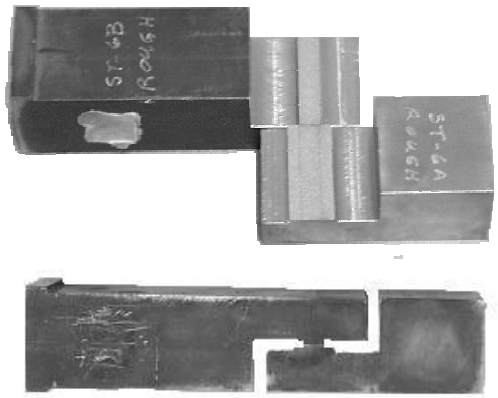

Figure 15. *Stepped specimen from which the data for the following figure (Figure 16) was obtained.*

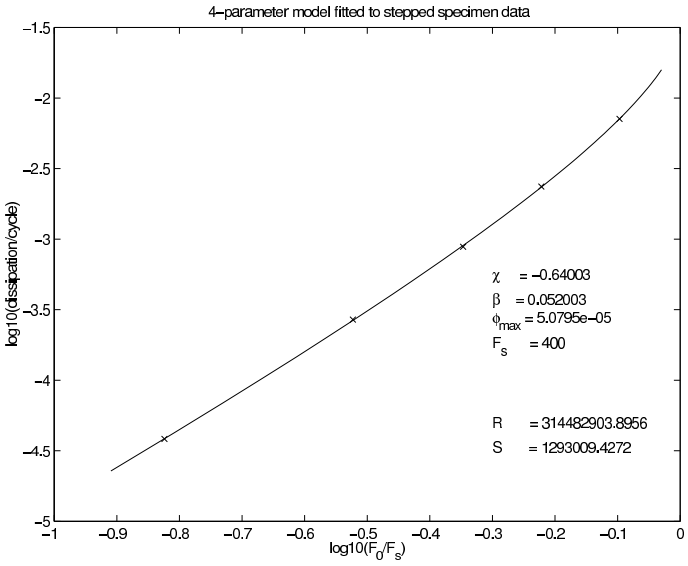

Figure 16. *Fit to dissipation data from a stepped specimen using an optimization method within Matlab.*

CURRENT STATUS OF IWAN MODELING

- The algorithm discussed above to fit experimental dissipation data has been extended to capture the joint stiffness as well [14].
- That extended algorithm has been employed to find improved model parameters for the individual legs of the Campaign 6 mock W76 AFF [14].

PLANNED RELATED ACTIVITIES

- A three legged mock W76 AFF will be subjected to transient excitation involving multiple modes. The experimental results will be compared with structural dynamics simulations where all three joints are modeled using the parameters discussed above.
- Research has begun on formulating a generalized model capable of accommodating multi-directional loading histories such as shear in two directions as well as bending.

Hysteresis Models

A simple model that will yield a power law relationship is given by the following.

For an increasing displacement

$$F_u = k\,(d - d_i) - k_n\,(d - d_i)^n + F_i \tag{16}$$

where k is a linear stiffness term, d is the displacement, d_i is the displacement at the last displacement reversal, k_n is a nonlinear stiffness, n is a nonlinear exponent, and F_i is the force at the last reversal.

For a decreasing displacement

$$F_d = -k\,(d_j - d) + k_n\,(d_j - d)^n + F_j \tag{17}$$

The values at the reversals are given by

$$F_j - F_i = k\,(d_j - d_i) - k_n\,(d_j - d_i)^n \tag{18}$$

Equations 16 and 17 can be written as a single equation as

$$F - F_i = \text{sgn}(d - d_i)\left(k\left|d_i - d\right| + k_n\left|d_i - d\right|^n\right) \tag{19}$$

At the force and displacement reversals

$$F_u(d_i) = F_d(d_i) = F_i \text{ and } F_u(d_j) = F_d(d_j) = F_j \tag{20}$$

The forces and displacements match at the displacement reversals. The slope of the force/displacement is

$$F'_u = k - nk_n\left(d - d_i\right)^{n-1} \text{ and } F'_d = k - nk_n\left(d_j - d\right)^{n-1} \tag{21}$$

where the prime denotes differentiation with respect to displacement. At the displacement reversals the slopes are

$$F'_u(d_i) = F'_d(d_j) = k \text{ and } F'_u(d_j) = F'_d(d_i) = k + nk_n(d_j - d_i)^{n-1} \tag{22}$$

Thus the displacement/force curve is symmetric and matches the desired slopes at the displacement reversals. Figure 17 illustrates the model. The energy loss/cycle for a cyclic input is found by integrating the force/displacement around one cycle of the hysteresis and is given by

$$E = k_n\left(\frac{n-1}{n+1}\right)\left(d_j - d_i\right)^{n+1} \tag{23}$$

The parameters can be solved from the above equations. If $n = -1$, the energy loss is not a function of input displacement, clearly a degenerate case. If $n = 1$, the system is linear and the nonlinear term is not needed. One deduces n from the slope of $log(E)$ vs. $log(d)$. In general, one obtains sensible model behavior for $1 \leq n \leq 2$. The other parameters are

$$k_n = E\left(\frac{n+1}{n-1}\right)\left(d_j - d_i\right)^{-(n+1)} \tag{24}$$

$$k = \frac{\left(F_j - F_i\right) + k_n\left(d_j - d_i\right)^n}{d_j - d_i} \tag{25}$$

For the stiffness model the slope of the force/displacement function will be negative if the absolute value of the displacement exceeds

$$\left|d - d_i\right| = \left(\frac{k}{nk_n}\right)^{\frac{1}{n-1}} \tag{26}$$

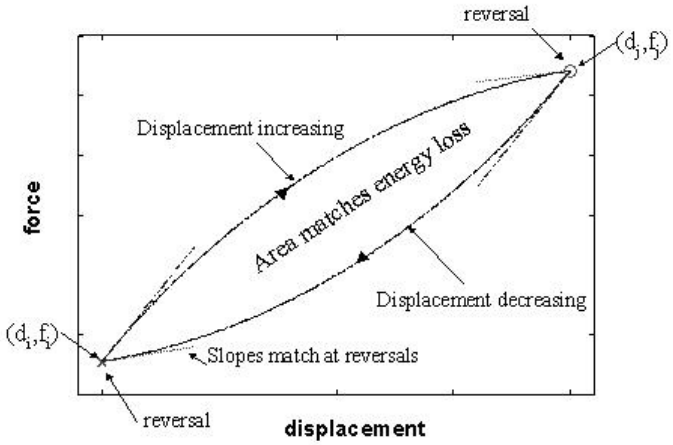

Figure 17. *Stiffness model*

$$|F - F_i| = k\left(\frac{k}{nk_n}\right)^{\frac{1}{n-1}} - k_n\left(\frac{k}{nk_n}\right)^{\frac{n}{n-1}} \tag{27}$$

If the displacement limit is reached, the force can be set to the limit force. The limit force can also be bounded by a coefficient of friction times the normal force as discussed in the next section. All the parameters of the model can be determined by performing tests with a periodic force input and measuring the energy loss/cycle as a function of the peak input force. The model will correctly predict the energy loss/cycle as long as a power law relationship exists between the input force and the energy loss.

To use this model one needs the following information: 1) The slope of the power law relationship to derive n, 2) the energy dissipated at one peak-peak displacement level to derive k_n. 3) The peak-peak relative displacement for a given peak-to-peak force to derive k.

To compute the force one needs to know: 1) the displacement, 2) whether the displacement is increasing or decreasing, 3) whether the displacement is larger or smaller than the displacement at the last displacement reversal, and 4) the displacement and

force at the last displacement reversal.

The equations can be written in a non-dimensional form as follows:

First normalize with respect to the force F_m expected to cause macro-slip. This can be expressed in terms of the normal force, N, and the coefficient of friction, μ:

$$F_m = \mu N \tag{28}$$

The displacement is normally dominated by the linear displacement term, hence a reasonable displacement for normalization is the displacement calculated from the linear term which will cause macro-slip.

$$d_m = \mu N/k = F_m/k \tag{29}$$

Equation 19 can now be written in a non-dimensional form as

$$\frac{F - F_i}{F_m} = \mathrm{sgn}(d - d_i)\left(\frac{|d - d_i|}{d_m}\right)\left(1 - \bar{k}_n\left(\frac{|d - d_i|}{d_m}\right)^{n-1}\right) \tag{30}$$

where

$$\bar{k}_n = k_n \frac{F_m^n}{k^{n-1}} \tag{31}$$

Normally

$$\bar{k}_n\left(\frac{|d - d_i|}{d_m}\right)^{n-1} << 1 \tag{32}$$

One more modification is needed to make the model useful. If the hysteresis curve crosses a previous hysteresis curve the reversal point must revert to the previous reversal. The following outlines the procedure.

Let $d_r(j)$ and $F_r(j)$ be a history of reversals, where j is the latest reversal. The reversals will alternate between the displacement changing from increasing-to-decreasing and decreasing-to-increasing. Let $d(i)$ be the latest displacement.

If $F/F_m > 1$we have macro-slip and the force is set to $F = F_m\mathrm{sgn}(F)$.

If the displacement is increasing ($d(i) > d(i-1)$) and $d(i) > d_r(j-1)$, or if the displacement is decreasing ($d(i) < d(i-1)$) and $d(i) < d_r(j-1)$, then

$$F_r(j) = F_r(j-2)\,\text{and}\,d_r(j) = d_r(j-2) \tag{33}$$

This is illustrated in Figure 18.

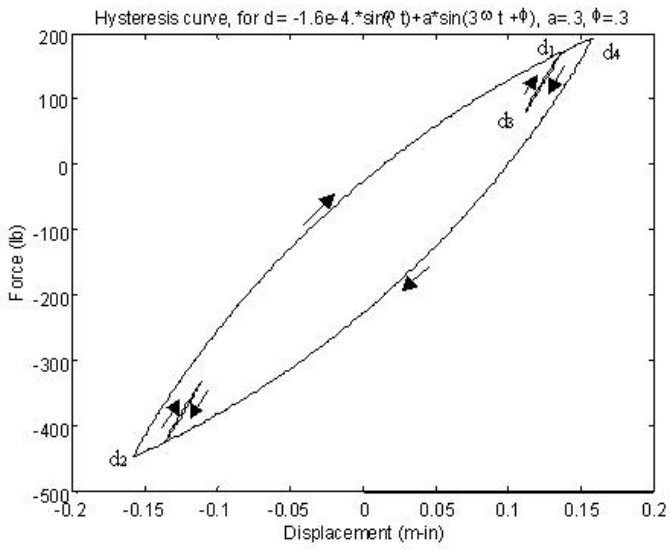

Figure 18. *Hysteresis for waveform with third harmonic added*

Generalization to include parameters which are a function of the normal force

The model can be generalized to include parameters that are simple functions of the normal force as follows. For the stiffness model let the parameters be a polynomial function of the normal force, N.

$$k = \sum_{m=0}^{M_k} A_m N^m \ , \ k_n = \sum_{m=0}^{M_{kn}} B_m N^m \ \text{ and } \ n = \sum_{m=0}^{M_n} C_m N^m \tag{34}$$

Normally only a very few terms will be included in the sums, probably 0, 1, or 2 at most. If $M_k = M_{kn} = M_n = 0$, the model becomes the stiffness model discussed earlier.

Compliance Model

Smallwood has also developed a similar model based on compliance instead of stiffness. This nature of the model is similar to the stiffness formulation and is fully documented in [16].

Measurement of the model parameters from experiments

In a normal experiment the joint is in series with another structure. It is assumed that the experimental structure exclusive of the joint can be modeled as a linear stiffness, k_s . The stiffness of the joint is modeled as, k_j. The stiffness of the combined system is k_c. Appropriate experiments can usually measure k_s and k_c , but rarely k_j . Assuming the elements are in series allows the stiffness of the joint to be calculated from

$$k_j = \frac{k_c k_s}{k_s - k_c} \tag{35}$$

Application to Specific Configurations

The whole-interface models discussed above are designed in a manner that involved local relative deformations. Such a formulation can be used in a finite element context to capture more distributed contacts.

In Figure 19 we see a circular plate clamped around its periphery. Also shown formally is a partition of the nodes on and near the periphery into groups that can be constrained into components of whole-interface joints. Such multi-point constraints (MPCs) are common in conventional finite elements, though they are usually awkward to apply.

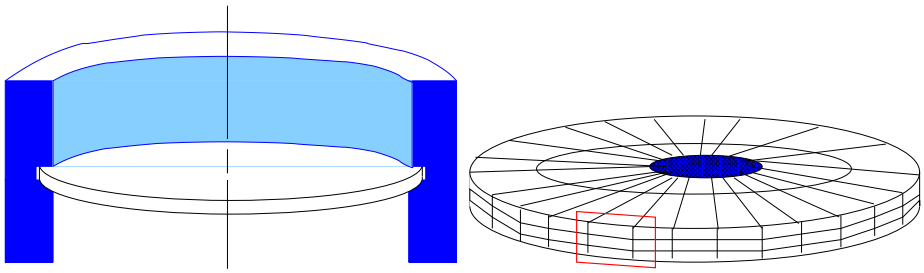

Figure 19. *A distributed jointed connection can be approximated as a distribution of whole-interface models.*

Uncertainty Quantification

For reasons discussed below, each joint model form must be accompanied by an associated quantification of the uncertainty of calculations based on that model. The following addresses this issue in the context of the parallel-series Iwan model, but similar analysis can and must be done for any other joint model used in predictive structural mechanics.

The form of the Iwan model described in this report is a deterministic framework for simulating the dynamic behavior of mechanical lap joints. The current model is cast in a four-parameter form, and it is hoped that it can accurately simulate mechanical response and energy dissipation in joints. When either the external force on the joint or the external joint deformation is specified, then the non-specified quantity can be computed, and the two can be used to compute the energy dissipated in the joint.

Of course, when either the force or deformation is specified as a deterministic signal, then the other quantity is deterministic, and the energy dissipated is reckoned a deterministic quantity. This deterministic construct may be satisfactory under many circumstances, however, real joint behavior is stochastic, and when the level of stochasticity is relatively large, then it must be accounted for in modeling and analysis. This stochasticity is reflected in measurements taken during physical experiments. Some of the stochasticity arises from reducible sources, and the remainder from irreducible sources. For example, one ever-present source of reducible randomness is transducer measurement error. All measurements are contaminated with noise that arises from electro-mechanical sources. Most of the data reduction procedures in use today seek to diminish the effects of this noise source with increasing numbers of measurements or measurement duration.

There are many sources of irreducible randomness, but usually, the most substantial source is termed "unit-to-unit variability." Every structural system that consists of an ensemble of realizations of nominally identical elements is actually composed of elements that differ in their details. Sometimes these differences are great and sometimes small. Sometimes the differences are reflected strongly in specific measures of behavior and weakly in others. Nevertheless, they are always present. Experiments on relatively simple structures have shown that unit-to-unit variability is the single source that contributes the most to structural randomness [1].

It is anticipated that mechanical joints are random in nature, and indeed, it is thought that they may be the major contributors to the randomness that arises from unit-to-unit variability. In view of this, it is important to represent this randomness

in the Iwan (or other) model for mechanical joint behavior. This can be accomplished by making the four parameters of the Iwan model random variables. In general, the four model parameters R, S, χ, and $\phi_{\max}$ specified in Eq. 7, can be assumed random. (Alternatively, one could as well work with parameters F_S, β, χ, and $\phi_{\max}$.) The most complete specification identifies their joint probability distribution. Any sufficiently specified form of a stochastic Iwan model would be capable of generating a plausible realization of mechanical joint behavior consistent with experimental results. Further, a probabilistic model should be capable of establishing probabilistic joint behaviors derivable from the parameters.

Though the most complete specification of the Iwan model identifies the joint probability distribution of the model parameters, the resources for accomplishing such a specification via the methods of statistics may not exist. Therefore, a partial, or approximate, probability model may provide the only practical alternative. Such a probability model might consist of the marginal probability distributions of the individual Iwan model parameters, along with the matrix of correlations between pairs of parameters. A model containing less information, and one that would be easier to specify, would simply specify statistical moments (say, first and second order) of the Iwan model parameters.

Because the Iwan model parameters may be non-Gaussian and strongly dependent, a useful approach to their probabilistic modeling may lie in the Karhunen-Loeve ([2]) approach to stochastic modeling. This approach, in effect, creates a decomposition for the Iwan model parameters that permits their expression in terms of a sequence of uncorrelated random variables. Whatever approach is taken to the probabilistic modeling of the Iwan joint, a statistical analysis that accounts for the limited experimental data used to identify the Iwan model parameters should be performed. The first investigation of the Iwan model will:

- Identify the parameters of the Iwan model from experimental data.
- Perform second-order statistical analysis on the parameter realizations.
- Specify a moment-based probability model with the results.

The above discussion has been fairly general in nature. As the modeling effort is refined, the effort in uncertainty quantification will be refined also. As the uncertainty quantification effort matures, it will provide tools necessary to initiate a rigorous validation effort.

Special Interface Models

The whole-interface models are the most sophisticated joint modeling tool available at this time and offer capabilities for modeling of structures that have not existed up to this time. On the other hand, one can list the limitations of this approach and seek an approach that is not subject to those limitations. Among the limitations of whole-interface elements are

- The constitutive parameters are selected to reproduce the experimental (or minutely simulated) behavior of that specific joint under a specific type or blend of specific types of load history. In this sense the answer has to be known in advance.
- With the multi-point constraints imposed on each side of the interface, stress recovery in the joint and interface is precluded.
- This approach, developed for lap-type joints, would be difficult to generalize to other classes of joint.
- Implementation of this approach, though possible via Lagrange multipliers or penalty functions in standard finite element architectures, is awkward to implement.
- This approach is also awkward for the analyst, who must define the MPCs and specify the governing equations to connect them.

One general strategy to overcome the above limitations would involve a class of interface elements that capture the artifacts of micro-slip without employing the micro-size mesh necessary to follow those kinematics. The strategy envisioned here is one where instantaneous normal traction is used as a proxy for the detailed kinematics of the evolving contact kinematics, thus indirectly capturing the kinematics identified by Heinstein and Segalman [8]. The constitutive nature of such interface elements is yet to be defined, but one can expect that among the parameters of the element will be the initial distribution of normal traction over the element and that the shear force/shear traction response of the element will be modulated by the dynamic loads seen at its nodes. Some of this vision is illustrated in Figure 20.

Of course, this approach can only be meaningful if the special interface elements converge; as one refines the mesh, the predicted structural response converges to that of a very finely meshed conventional finite element analysis.

The first challenge is to find a constitutive model that is capable of yielding the appropriate dissipation behavior as shear and normal tractions are varied in a coordinated manner .

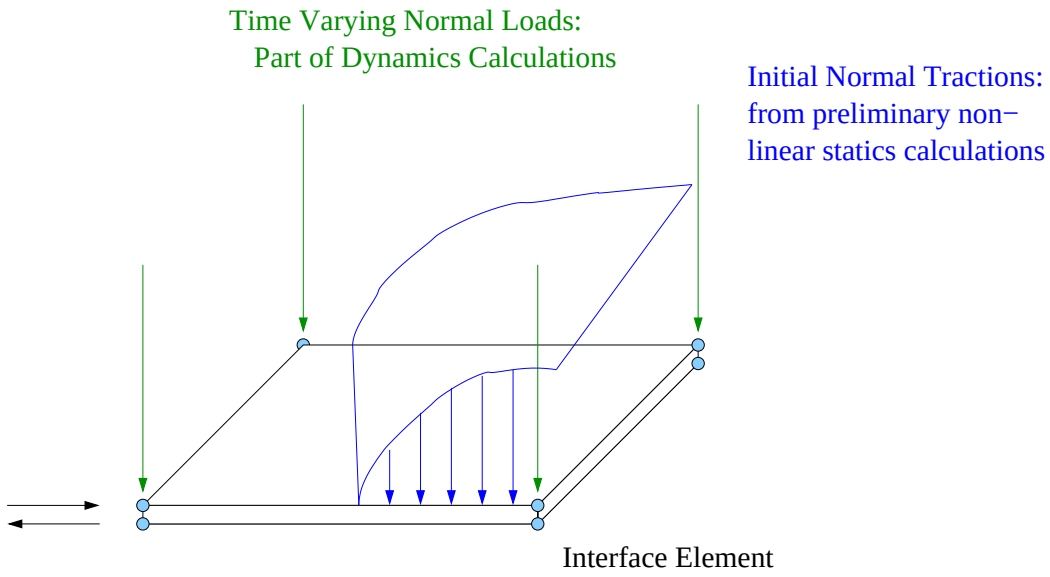

Figure 20. *Scheme for special interface elements to capture micro-macro slip employing a relatively coarse mesh.*

Iwan Series-Series Illustration

One very simple candidate constitutive model that might serve as a basis for the interface model is a series-series model such as shown in Figure 21. This series arrangement of Jenkins elements opposing a series arrangements of elastic elements was never explicitly considered by Iwan, but it is in the same spirit of the parallel-series Iwan systems discussed earlier.

Because of the spatial distribution of the Jenkins elements, a distribution of normal traction over an element is also seen among the ordered Jenkins elements. If one assumes that the strength of each slider is proportional to a local normal traction, the response of this system is seen to be modulated by any time-varying spatial distribution of normal tractions. (See Figure 22.)

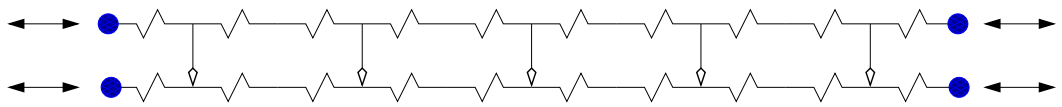

Figure 21. *The series-series Iwan model is the basis for one possible interface model.*

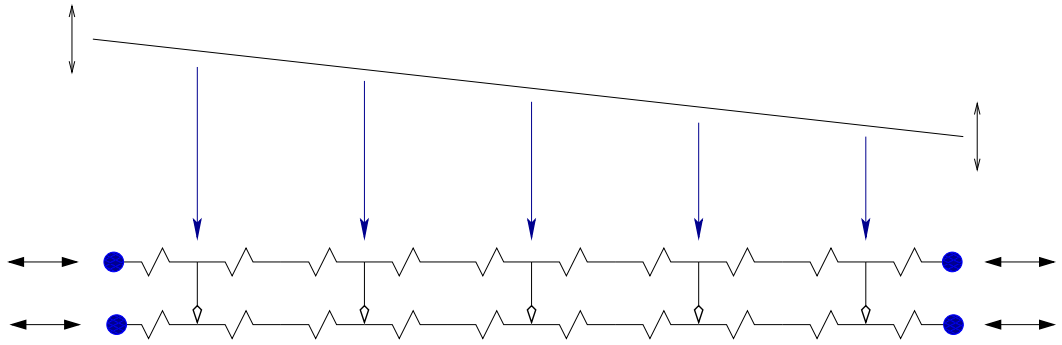

Figure 22. *Spatially varying normal tractions result in corresponding distributions of slider strength among the Jenkins elements.*

Preliminary calculations indicate that a spatially linearly varying normal traction distribution acting on top of a steady uniform distribution and changing synchronously with shear loads on the boundaries will result in the fractional power-law energy distribution that one associates with joints.

In one implementation, the series-series systems would be placed between every pair of Gauss quadrature points in the interface element (Figure 23). Displacements would be interpolated from the nodes to the quadrature points in the usual manner. The normal and shear tractions would be mapped from the quadrature points to the nodes in the standard manner.

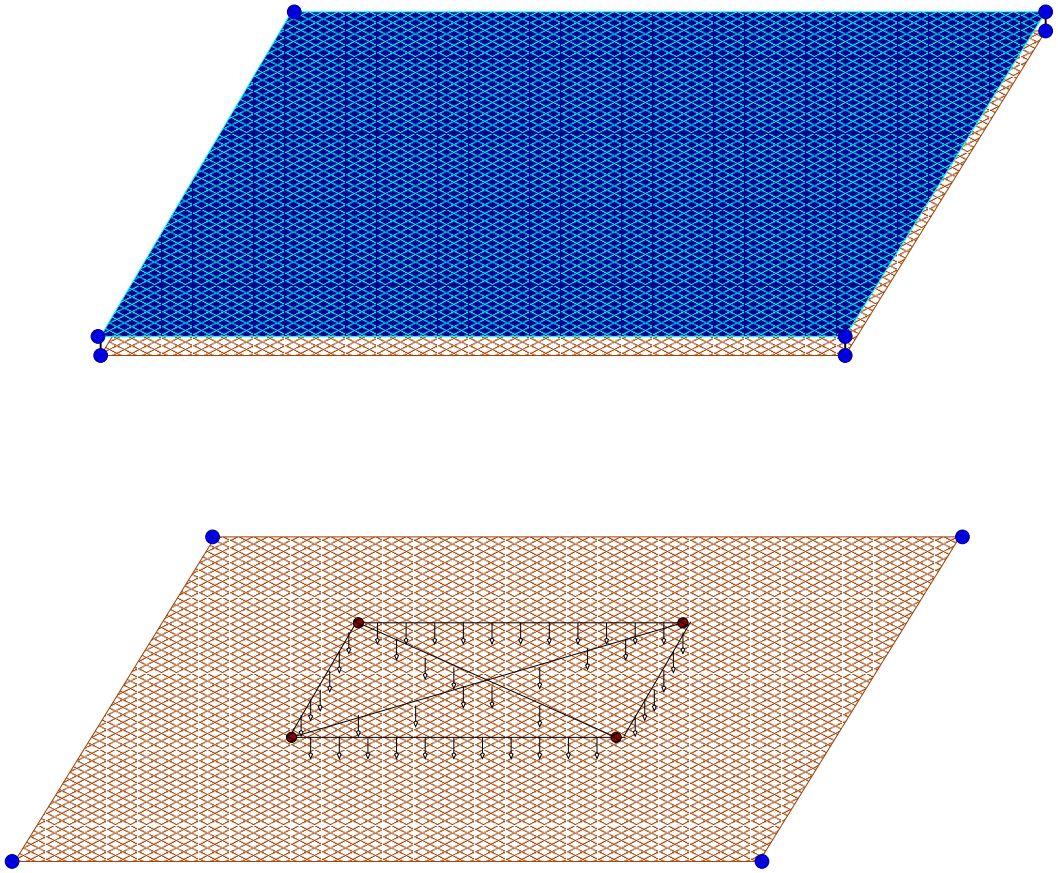

Figure 23. *An interface element would be created from series-series Iwan systems spanning each pair of quadrature points.*

The strategy suggested here, using series-series Iwan systems, is supported by

some encouraging preliminary calculations, but it is presented here primarily for the purpose of illustration. It will probably be one of many approaches that will be explored.

It should be mentioned that series-series Iwan systems could have been considered for whole-interface modeling in much the same manner that parallel-series Iwan models were employed. On the other hand, the series-series systems offer a special advantage in building the above sort of interface element - they explicitly account for spatial gradients in the normal tractions. It does not appear that such a dependence could be built into the parallel-series models.

Advantages of the Special Interface Element Concept

Special interface elements - if devised to have the features described above - would have substantial advantages

- These elements should capture the necessary physics of joints in a manner employing elements of size comparable to those elements used to capture the rest of the structure.
- This strategy should be general enough to capture a broad range of joint configurations such as generalized lap joints as well as tape joints (Figures 24 and 25).
- This strategy should be able to capture joint response to general load histories.
- There is nothing to preclude stress recovery.

Though this strategy of special interface elements is currently only a vision, it is supported by encouraging preliminary calculations and by the existence of numerous more candidate constitutive models arising from metal plasticity that could be core of workable strategies.

Threaded Joints

Threaded joints are a major part of the assembly of re-entry vehicles (RVs) as well as other structures of general interest. They are not only a major component of the

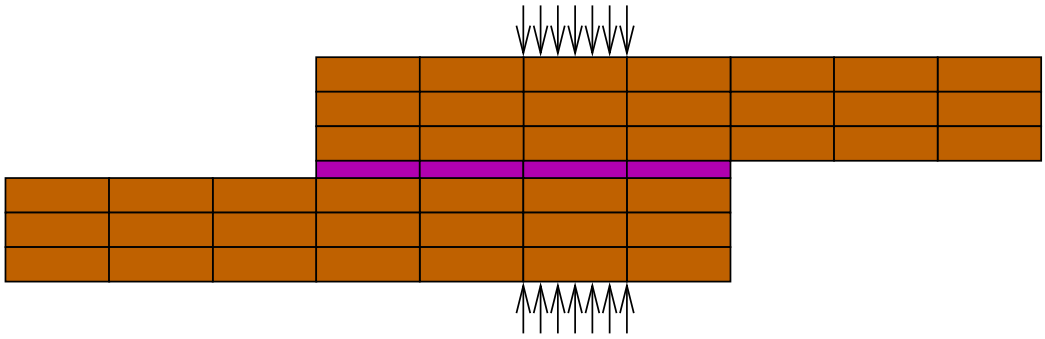

Figure 24. *Interface elements could be integrated into the modeling of generalized lap joints in a natural manner.*

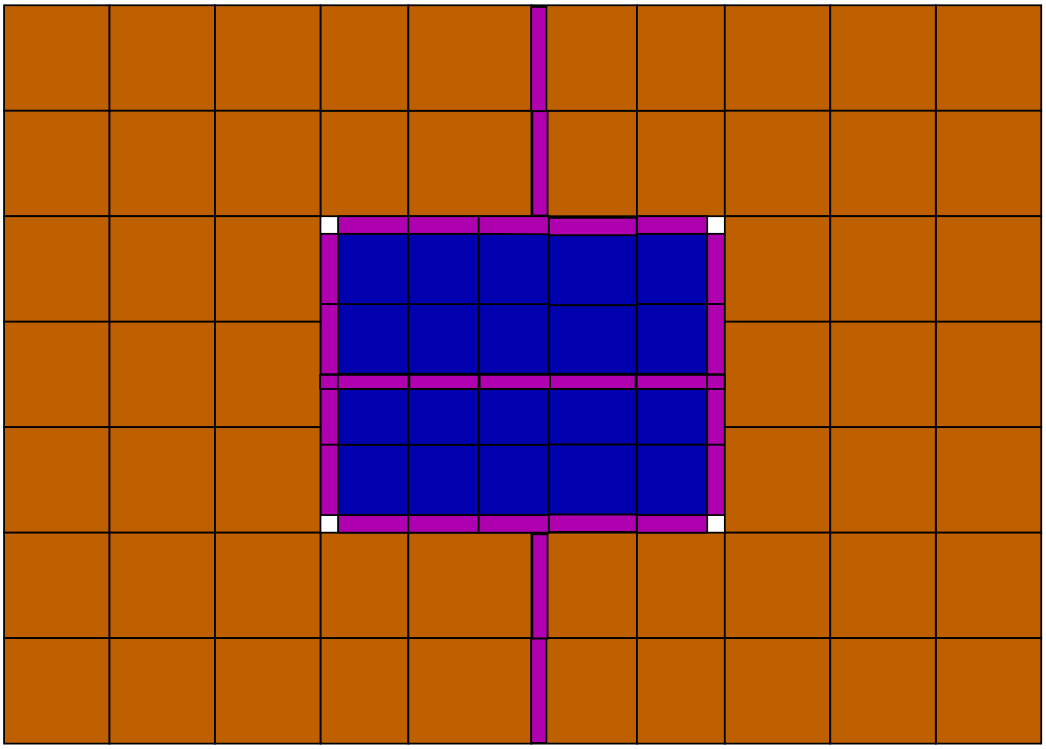

Figure 25. *Interface elements could be integrated into the modeling of tape joints in a natural manner.*

mechanical integrity of the structure, but also a major path for mechanical energy flow through the system. In fact, the energy flow through a threaded joint might be a more important factor than mechanical energy dissipation since it is generally believed that there is very little energy dissipation in tightened threaded connections. (See [7] for an example.)

As is the case generally for joints, very finely meshed finite element analysis of joints can lend insight into joint mechanics and can even be used to deduce parameters for lower order models, but such fine meshes would be impractical for direct use in structural dynamics modeling. The scale of the resolution necessary to capture threaded joint mechanics with conventional finite element analysis is indicated by the mesh in Figure 26.

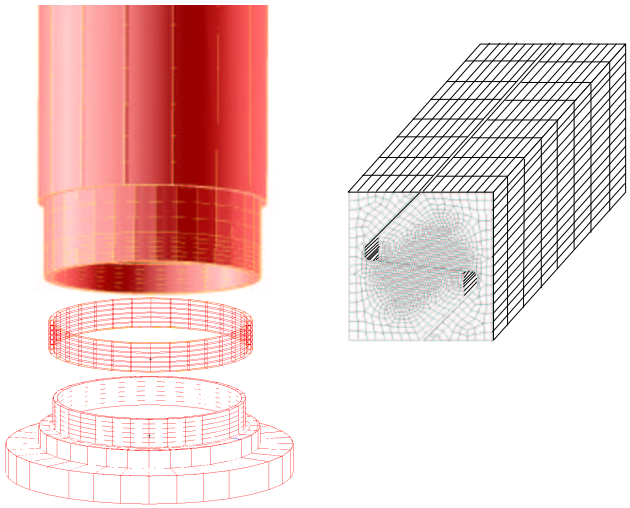

Figure 26. *Approximate mesh refinement necessary to capture detailed thread interactions.*

Since there is very little quantitative data on energy dissipation of threaded connections, the initial effort in threaded joint modeling focuses on

- capturing the manner in which statically indeterminate equilibrium is achieved

in a threaded joint

- quantitatively representing the manner of mechanical energy transmission through the joint
- predicting the energy dissipation in some rational manner.

Clearly this modeling effort must occur along with an active program of experimental investigation and validation.

The geometry of most immediate interest to Sandia's mission is that of buttress threads (Figure 27). Insight into the joint mechanisms is obtained by performing finite element analysis (Figure 28) on a plain-strain representation for a single thread pair. When we constrain horizontal motion of the right and left sides of the thread pair and pull down on the member on the right and pull up on the member on the left, we obtain the normal and shear stresses shown in Figures 29 and 30. We see that the normal traction has the anticipated singularities at the edges of the contact patch. The shear stress is nearly uniform within the contact patch.

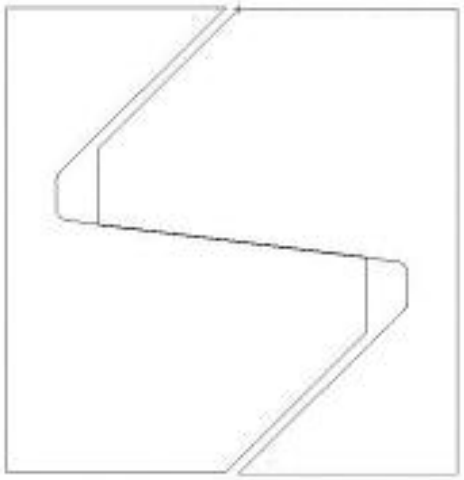

Figure 27. *Opposing buttress threads in joint.*

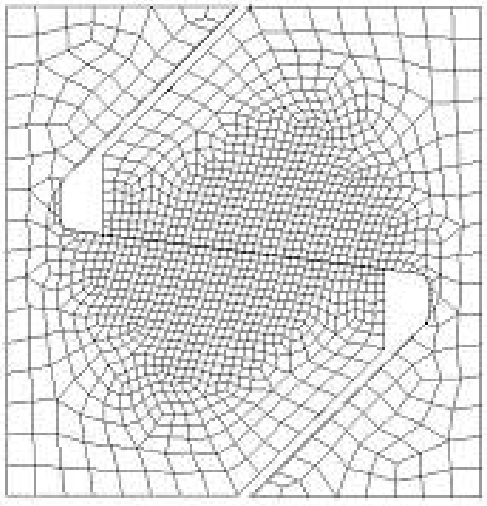

Figure 28. *Corresponding finite element mesh.*

We look for a simple, low order model that captures the general behavior generated by the detailed finite-element model discussed above. We have considered two

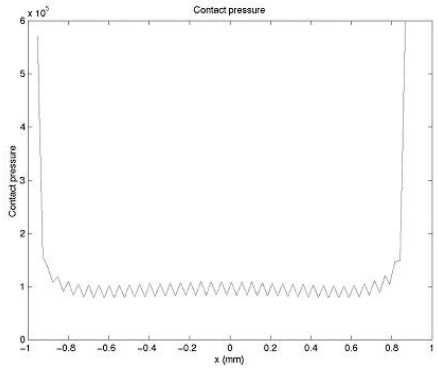

Figure 29. *Pressure across thread interface.*

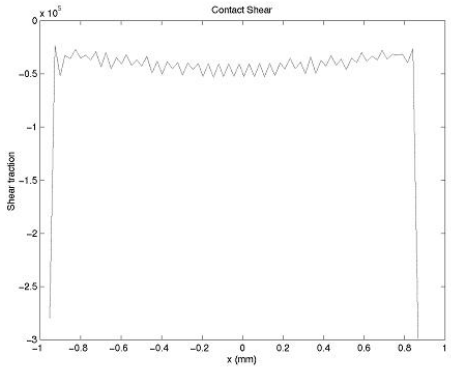

Figure 30. *Shear stress across Thread Interface.*

approaches

- *Thread Model T0* Here we consider a four node quad element (8-node hex in 3-dimensional analysis) whose nodal displacements correspond to those of the corners of a unit thread pair. This elastic element will have the properties of the thread pair if the thread interface is 'welded'. (See Figure 31) It is anticipated that this approach can be implemented in a straight-forward manner and will be manifest in ASCI code in FY03. In the near term, implementation in analysis will involve a laborious process of specifying properties of equivalent anisotropic material. Later, a special element will be coded for which most of those specifications will be done automatically.

- *Thread Model T1:* For this we have begun investigating the low-order model shown in Figure 32. This model - involving rigid components, preloaded sliders, linear springs, and uni-directional springs - does have the gross deformational features and normal traction stress concentrations predicted by the finite-element model. The finite element results indicate a nearly uniform shear stress over the contact patch due to the specified loading; the two discrete sliders should result in identical dissipation so long as the shear stress varies linearly over the contact patch.

  It has not yet been determined how to map this low order model into a finite element of conventional topology, and that is one of the foci of current research.

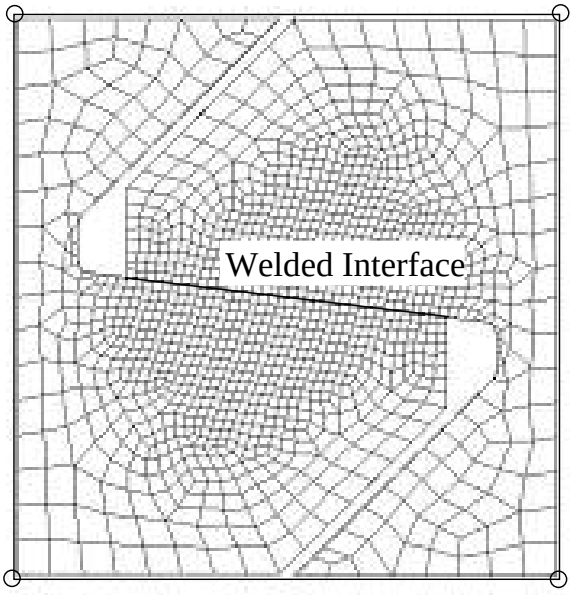

Figure 31. *The T0 element is created to have the same elastic properties of a thread pair unit when the thread interface is 'welded'*

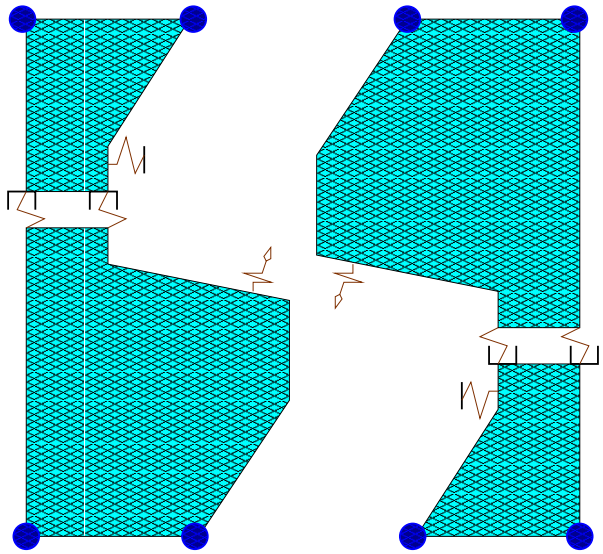

Figure 32. *Reduced-order model(T1) for unit-cell of thread pairs. Nodes indicated in blue are sufficient to define internal thread deformation.*

The two-dimensional thread-pair models indicated in Figures 31 and 32 can be projected into three dimensional elements (Figure 33). If these elements are projected so as to be quadratic in the circumferential direction, one imagines that as few as several dozen circumferential elements would be sufficient for each layer of thread elements. If the elements are projected so as to be linear in the circumferential direction, many more elements would be required.

The very coarse modeling strategy described above should have the advantage of adding only a tractable number of nonlinear equations to the total system of equations. Additionally, this strategy should reproduce the properties of threads to the extent that those properties are currently understood.

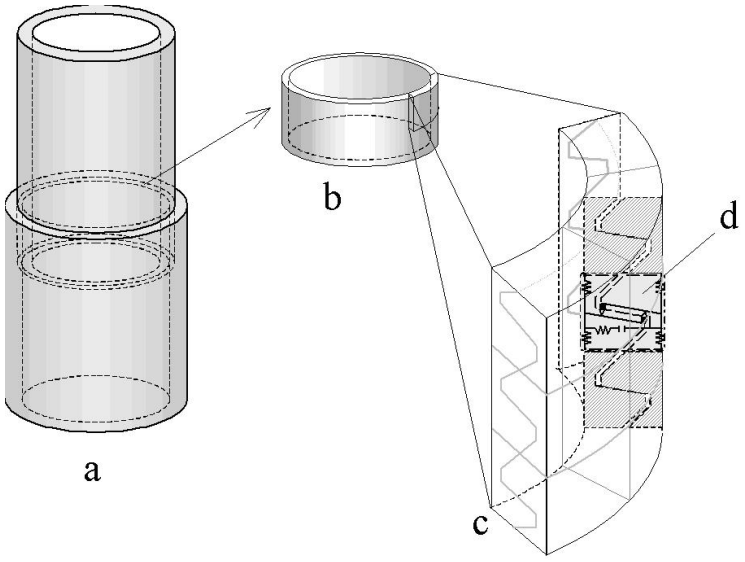

Figure 33. *Axi-symmetric application of reduced order thread interface elements.*

Finally, one should observe that while determining the parameters of the low-order thread-models by reference to a detailed finite element model, we can also express failure related quantities of the thread (such as stress intensity factor) in terms of the internal degrees of freedom of the low-order model. In this manner, we can create a facility within a structural dynamics code to flag when threads go through a failure load.

Of course, this program must also take place along with corresponding programs of experimental investigation and validation. Some perspective of this is obtained by

observing that the detailed finite element models from which low-order models will be derived are themselves not yet validated.

Slap/Gapping Modeling

Slapping and gapping are processes that can be expected in most weapons systems, but they are generally expected in environments of high amplitude excitation. Slapping is observed most strongly through indirect evidence: when a built up structure is subject to high amplitude but frequency limited excitation, the measured accelerations at the far side of the structure include components at much higher frequencies.

Several ASCI codes (Adagio, Andante, Presto) have slap/gapping features built in as core features of the code and similar features are being added to Salinas. Because current codes (including the ASCI codes) address slapping through direct time integration, their time steps must be exceedingly small and their meshes exceedingly fine. It is therefore prohibitive to compute the high-frequency response of continuing slapping processes over long times (seconds). This topic would appear to be very fertile for a new mathematical formulation.

Another flavor of this problem has to do with gaps opening up and closing on a slow time scale, modulating stiffness of the structure as seen by higher frequency events.

These are important but difficult issues. Major efforts will focus on addressing them as more urgent, slip-related milestones are accomplished.

Experimental Program

This document focuses on the road map of the joints modeling effort, but some words must be said about the experimental program since so much of the progress of the modeling is contingent on experimental results.

Basic Experiments (ESRF)

Fundamental research experiments funded under Engineering Sciences Research Foundations have been collecting dissipation data on lap-type joints for several different

geometries. This data has been used in developing the constitutive models discussed above. This work is continuing with a focus on part-to-part variability and issues of repeatability. Also, a broadening range of joint geometry is being addressed. Each of these experimental programs is accompanied by detailed quasi-statics and structural dynamics calculations to assure that the computational tools account for all the physics manifest in the experimental results. Shown in Figure 34 is the basic test configuration for much of this research.

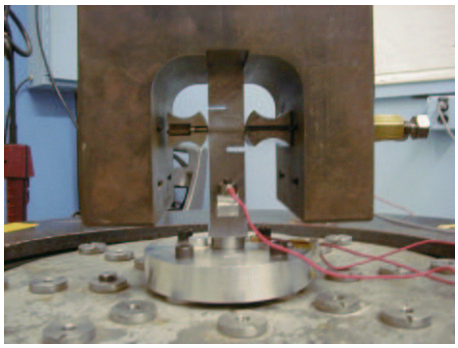

Figure 34. *Basic lap joint test configuration.*

Mock W76 AFF Campaign 6 Experiments

The Campaign 6 (C6) program was created to validate the ASCI models against realistic approximations to true weapons systems as well as to perform discovery experiments and qualification-like tests on representative hardware. A mock W76 AFF was created to test the three major types of joints that occur on that system: bolted, threaded, and tape joints. There are three separate C6 tasks - all associated with the Verification and Validation effort - to address these three joint types. The experimental program has progressed in all three directions. Shown in Figures 35 and 36 are the test articles for the bolted and threaded joints, respectively.

The lap-joint modeling effort is the most advanced, so the validation effort is also most advanced in addressing the modeling of that sort of joint.

Figure 35. *Mock AFF test assembly*

Figure 36. *Threaded shell and AFF base.*

Milestones

With the exception of the formal Level II mileposts, the dates associated with milestones presented below are no more than a current best-estimate of when the tasks will be completed. They do not have extra leeway inserted to accommodate the uncertainties intrinsic to the research effort and should therefore be viewed as optimistic. The detail is presented to show a coherent picture of the strategy, but the individual tasks are subject to re-sorting and re-structuring as the situation evolves.

In what follows, in order to avoid ambiguity, the term 'model' refers to a constitutive model. Depending on context, 'model' may also refer to the implementation of that constitutive model in code. We use the term 'model specification' to refer to the use of the constitutive model plus specific model parameters to reproduce the behavior of a particular piece of hardware.

Due Date	Task	Funding Sources
2002, Q4	Whole Joint Models Introduced to Salinas: *Done*	M&PM, V&V
2003, Q3	Sandia Report on Whole-Joint Modeling, How To Employ It, And Its Implementation In At Least One Of The ASCI Codes (Level II M&PM)	M&PM, V&V
2003, Q4	Salinas with Whole-Joint Models Employed in a Weapons Analysis	M&PM, V&V
2003, Q4	Threaded Joint Model (T0) Ported to Salinas	C6, ESRF, V&V
2003, Q4	A Bolted Joint Model Specification Implemented in Salinas and Validated Against Experimental Data Of The Single Jointed Leg (Level II V&V)	C6, M&PM, V&V
2004, Q1	Iwan Whole-Interface Model Extended to Accommodate Loads that Achieve Macro-Slip	C6, ESRF, V&V
2004, Q3	Whole Joint Models Generalized to Accommodate Multiple Loading Modes	ESRF, M&PM
2004, Q3	Documentation on Uncertainty Analysis of Whole-Joint Model for Mock W76 Bolted Leg Joint	M&PM & V&V
2004, Q4	Whole Joint Models Introduced to Adagio and Presto	M&PM, V&V
2004, Q4	Threaded Interface Model (T1) Ported to Salinas	ESRF, V&V
2005, Q1	AFF Hostile Environment Test (V&V milepost 5.1)	V&V
2005, Q4	Threaded Joints Introduced To Adagio And Presto	M&PM, V&V
2006, Q4	Consistent Formulation for Interface Element With Appropriate Constitutive Equation Documented	M&PM, V&V
2007, Q2	Initial Generalized Tape Joint Model in Salinas	C6, ESRF, V&V
2008, Q2	Interface Elements for Joints in Salinas	ESRF, M&PM, V&V

Closing

The road map presented above shows a variation in detail and resolution from place to place reflecting the current levels of effort in each aspect of the problem. It is anticipated that as the research effort progresses and as our understanding of each joint-related topic matures, the planning process will have more resolution in some areas and changed perspectives in others. Additionally, as new strategies arise and are weighed against those currently envisioned, the road map directions will be modified appropriately. For these reasons, it is expected that this document will undergo periodic formal revisions.

One of the areas for which the road map will be refined further as the research effort matures has to do with the intrinsic probabilistic nature of joint mechanics. Because of that nature of joints, the ultimate goal of the joint modeling effort will include the formulation and implementation of models that yield probabilistic predictions as well as the formulation of methods to validate those probabilistic models.

Finally, a few comments should be made about the essential etiology of joint mechanics. As discussed in Section above, joint mechanisms cannot be observed directly. In other topics for which this is the case, a "first principles" understanding tends to come *last*, and the evolution of understanding occurs in the following broad steps:

- A large number of experiments or observations is performed to obtain a general and qualitative understanding of the underlying phenomena.
- Eventually sufficient study of the above observations yields to simple descriptive equations that capture a preponderance of the trusted data.
- Finally, once the relevant research community has had time to digest the descriptive equations, it hones its understanding of the underlying physics to develop "first principles" explanations.

Such was the story of metal plasticity. The first names in the literature are experimentalists who documented the phenomena (such as Ludwik, G. I. Taylor, and Orowan). The next slew of investigators who impacted metal plasticity were those who captured the experimental observations in empirical constitutive equations (such as Westergaard, Prager, and Drucker). The dislocation theory of metal plasticity came last. (A similar evolution is associated with celestial mechanics: Brahe $\rightarrow$ Kepler $\rightarrow$ Newton).

The above discussion of etiology suggests that investigation of joint mechanics will have a similar evolution. The development of suitable joint models requires not only a process of systematic investigation, but also the search for suitable concepts.

References

[1] R.J. Aumann, A. S. McCarty, and C. C. Olson, Identification of Random Variation in Structures and Their Parameter Estimates, *Proceedings of the XXI International Modal Analysis Conference,* Orlando, Florida, 2003

[2] R. Ghanem and Spanos, *Stochastic Finite Elements: A Spectral Approach,* Springer-Verlag, New York, 1991

[3] L. Gaul and S. Bohlen, The Nonlinear Transmission Behavior of Joints, *Zeitschrift fur Angewandte Mathematik und Mechanik, v. 64*, No. 4, pp. T45-T48, 1984

[4] L. Gaul, J. Lenz, Nonlinear Dynamics of Structures Assembled by Bolted Joints, *ACTA MECHANICA, 125*, No. 1-4, pp. 169-181, 1997

[5] M. Hanss, S. Oexl, L. Gaul, Identification of a bolted-joint model with fuzzy parameters loaded normal to the contact interface, *Mechanics Research Communications 29* pp. 177-187, 2002

[6] D. L. Gregory, D. O. Smallwood, M. A. Nusser, R. G. Coleman, Experimental Device to Study the Damping in Bolted Joints, (DETC99/VIB-8190), presented at the 1999 ASME Design Engineering Technical Conferences, September 12-15, Las Vegas, Nevada, 1999. (Unfortunately, the report did not show up in the conference proceedings, but a copy of the paper can be obtained from the lead author.)

[7] N. R. Hansen, V. I. Bateman, R. G. Bell, and F. A. Brown, Shock Transmissibility of Threaded Joints, *Proceedings of the 67th Shock and Vibration Symposium, Vol I,* Monterey,CA, November 1996.

[8] M. W. Heinstein and D. J. Segalman, Bending Effects in the Frictional Energy Dissipation in Lap Joints, *SAND2002-0083*, Unlimited Release, Printed January 2002.

[9] W. D. Iwan, A Distributed-Element Model for Hysteresis and Its Steady-State Dynamic Response, *Journal of Applied Mechanics Vol. 33*, 1966, pp 893-900.

[10] W. D. Iwan, On a Class of Models for the Yielding Behavior of Continuous and Composite Systems, *Journal of Applied Mechanics Vol. 34*, 1967, pp 612-617.

[11] D. J. Mead, "Structural Damping and Damped Vibration", *Applied Mechanics Reviews, Vol. 55*, no 6, November 2002, R45-R54.

[12] M. Persson, *New Scientist, vol. 160* no. 2156, p.30, 1998 (http://fy.chalmers.se/ tfymp/Homepage/friction.html).

[13] D. J. Segalman, An Initial Overview of Iwan Modeling for Mechanical Joints, *SAND2001-0811*,Unlimited Release, March 2001

[14] D. J. Segalman, A Four-Parameter Iwan Model for Lap-Type Joints, *SAND2002-3828*, Unlimited Release, Printed November 2002

[15] D.O. Smallwood, D.L. Gregory, and R. G. Coleman, Ronald, Damping investigations of a simplified frictional shear joint, *Proceedings of the 71st Shock and Vibration Symposium* held in Arlington, VA, November 6-10, 2000 (SAND2000-1929C)

[16] D.O. Smallwood, D.L. Gregory, and R.G. Coleman, A Three-Parameter Constitutive Model for a Joint which Exhibits a Power Law Relationship Between Energy Loss and Relative Displacement, *72nd Shock and Vibration Symposium, Destin, FL, Nov. 2001.* (Available form SAVIAC).

DISTRIBUTION:

1 Prof. Adnan Akay
Mech. Engineering Dept.
Carnegie Mellon Univ.
Pittsburgh, PA 15213-3890

3 Prof. Lawrence A. Bergman
Univ. of Illinois
306 Talbot Lab
104 S. Wright St.
Urbana, IL 61801

1 Prof. Robert Carpick
Dept. Engineering Physics
1500 Engineering Drive
University of Wisconsin
Madison, WI 53706

1 Dr. Luise Couchman
Office of Naval Research
Ballston Centre Tower One
800 North Quincy Street
Arlington, VA 22217-5660

1 Dr. Scott Doebling
Los Alamos National
Laboratory, MS P946
Los Alamos, NM 87545

1 Professor Larissa Gorbatikh
Department of Mech. Engr.
Mech. Eng. Bldg.
The Univ. of New Mexico
Albuquerque, NM 87131

1 Dr. Steve Griffin
Boeing SVS
4411 The25 Way NE
Suite 350
Albuquerque, NM 87109

1 Dr. Jason Hinkle
Aerospace Engr. Sciences
Campus Box 429
Univ. of Colorado
Boulder, CO 80309-0429

1 Dr. Norman F. Hunter
Los Alamos National Laboratories
MS C931 ESA-MT
Los Alamos, NM 87545

1 Prof. Dan Kammer
Dept. Engineering Physics
1500 Engineering Drive
University of Wisconsin
Madison, WI 53706

1 Dr. Marie Levine-West
Jet Propulsion Laboratory
Science and Technology Development Section
4800 Oak Grove Drive
Pasadena, CA 91109-8099

1 Dr. Dean Mook
AFOSR/NA
4015 Wilson Boulevard,
Mail Room 713
Arlington VA 22203-1954

1 Prof. K.C. Park
Aerospace Engr. Sciences
Campus Box 429
Univ. of Colorado
Boulder, CO 80309-0429

1 Prof. Lee Peterson
Aerospace Engr. Sciences
Campus Box 429
Univ. of Colorado
Boulder, CO 80309-0429

1 Dr. Chris Pettit
AFRL/VASD,
Bldg. 146, 2210 Eighth St.,
Wright Patterson AFB
OH 45433

1 Prof. Michael Plesha
Dept. Engineering Physics
1500 Engineering Drive
University of Wisconsin
Madison, WI 53706

1 Prof. D. Dane Quinn
Department of Mech. Engr.
College of Engr.
The Univ. of Akron
107b Auburn Science and Engr. Center
Akron, OH 44325-3903

1 Professor Henry Schreyer
Department of Mech. Engr.
Mech. Eng. Bldg.
The Univ. of New Mexico
Albuquerque, NM 87131

1 Professor Andrew Smyth
Columbia Univ.,
M̂ail Code 4709
500 West 120th Street
New York, NY 10027

1 Dr. W. Woytek Tworzydlo
Altair Engr., Inc.
7800 Shoal Creek Blvd, Suite 290E
Austin, TX 78757-1024

1 Dr. Y.C. Yiu
Lockheed Martin Missiles & Space
Organization E4-20 Bldg. 154
1111 Lockheed Martin Way
Sunnyvale, CA 94089

1 MS 139
Lott, Stephen E , 9905

1 MS 553
Bateman, Vesta I , 9126

1 MS 553
Smallwood, David O , 9124

1 MS 555
Garrett, Mark S , 9122

1 MS 555
Gregory, Danny L , 9122

1 MS 555
Stasiunas, Eric Carl , 9124

1 MS 557
Baca, Thomas J , 9125

1 MS 557
Carne, Thomas G , 9124

1 MS 557
Epp, David S , 9125

1 MS 557
Mayes, Randall L , 9125

1 MS 557
O'Gorman, Christian, 9125

1 MS 557
Paez, Thomas L , 9133

1 MS 557
Simmermacher, Todd W , 9124

1 MS 557
Sumali, Hartono , 9124

1 MS 557
Urbina, Angel , 9133

1 MS 824
Moya, Jaime L , 9130

1 MS 824
Ratzel, Arthur C , 9110

1 MS 828
Pilch, Martin , 9133

1 MS 834
Johannes, Justine E , 9114

1 MS 835
Alvin, Kenneth F , 9142

1 MS 835
McGlaun, J Michael , 9140

1 MS 835
Pierson, Kendall, 9142

1 MS 835
Walsh, Timothy , 9142

1 MS 841
Bickel, Thomas C , 9100

1 MS 847
Adams, Charles , 9125

1 MS 847
Attaway, Stephen W , 9134

1 MS 847
Bhardwaj, Manoj K , 9142

1 MS 847
Bitsie, Fernando , 9124

1 MS 847
Dohrmann, Clark R , 9124

1 MS 847
Fulcher, Clay W G , 9125

1 MS 847
Heinstein, Martin W , 9142

1 MS 847
Hinnerichs, Terry , 9126

1 MS 847
Hopkins, Ronald N , 9125

1 MS 847
Jung, Joseph , 9127

1 MS 847
Koteras, Richard, 9142

1 MS 847
May, Rodney A , 9126

1 MS 847
Mitchell, John A , 9142

1 MS 847
Morgan, Harold S , 9120

1 MS 847
Ozdoganlar, O Burak , 9124

1 MS 847
Red-Horse, John R , 9133

1 MS 847
Redmond, James M , 9124

1 MS 847
Reese, Garth M , 9142

10 MS 847
Segalman, Daniel J , 9124

1 MS 847
Starr, Michael J , 9124

1 MS 847
Walther, Howard P , 9125

1 MS 847
Wojtkiewicz, Steven, 9124

1 MS 893
Lo, Chi , 9123

1 MS 1110
Day, David M. , 9214

1 MS 1080
Dohner, Jeffrey L, 1769

1 MS 1159
Hedemann, Mark, 15344

1 MS 1360
Resor, Brian R , 9122

1 MS 1393
Chu, Tze Yao , 9100

1 MS 9042
Lauffer, James P , 8727

1 MS 9018
Central Technical Files, 8945-1

2 MS 0899
Technical Library, 9616

1 MS 0612
Review & Approval Desk, 9612